Progress In Electromagnetics Research Letters, Vol. 95, 83–90, 2021

A Broadband UHF RFID Tag Antenna Design for Metallic Surface Using Module Matching

Fei You and Zhi Jiang*

Abstract—In this paper, a broadband RFID tag antenna based on module matching is proposed, which is suitable for metallic surface. The antenna's 10-dB effective bandwidth covers 820–980 MHz. In order to achieve a more appropriate impedance matching in a wideband, a new technique of module matching to reach a wide frequency band is studied for realizing the consistent change of impedance between the antenna and the chip, and the frequency band is effectively widened. The feasibility of module matching to achieve maximum power transmission is analyzed. Further results demonstrate that the proposed tag antenna provides a stable gain when being mounted on metal plates of various sizes. In addition, the proposed design is cost-effective since it does not require metallic vias and has a compact size. The maximum reading distance at 910 MHz on the metallic surface is 4.5 m.

1. INTRODUCTION

Radio frequency identification (RFID) technology is widely used in logistics packaging tracking and supply chain management due to its strong anti-interference ability, long reading distance, and low cost [1, 2]. When UHF-RFID tags are directly connected to metallic surfaces such as metallic packaging, automobiles, and containers, they will change the antenna's gain, input impedance, and operating frequency, resulting in problems such as reduced gain and frequency detuning [3]. Hence, a tag placed near the metallic plane induces an image current of the opposite phase in the metallic surface, which dramatically degrades its antenna performance [4]. Some scholars studying microstrip patch antennas or PIFA antennas have proposed to use metallic surfaces as ground planes to improve the gain of tag antennas attached to the surface of metal objects [5–7]. However, these antennas need to have short-circuited walls or substrates containing metallic vias, making the manufacturing cost of such tags much higher than other types of labels. For tag antennas, regardless of etching technology or printing technology, planar antennas are facilitated by large-scale manufacturing, which makes the cost of tags as low as possible [8].

A typical UHF passive RFID tag is composed of an antenna and an RFID chip. Since the tag chip has a real part and an imaginary part of the impedance, to achieve maximum power transmission, the input impedance of the antenna must be conjugate matched with the impedance of the tag chip [9]. However, there is a problem of impedance mismatch for a wideband tag antenna. Literature [10] proposed to use double T-matching to achieve impedance conjugate matching on a broader frequency band, but its return loss is significantly increased in the UHF band, which shows that the multiple T-matching mode is also challenging to achieve full coverage of the conjugate matching in a wide frequency band.

The module matching mode is used in this letter to solve the impedance matching problem in a wide frequency band. The maximum power transmission characteristics of the tag antenna in the module

Received 17 September 2020, Accepted 5 December 2020, Scheduled 19 December 2020
* Corresponding author: Zhi Jiang (960358708@qq.com).
The authors are with the School of Communication and Art Design, University of Shanghai for Science and Technology, Shanghai 200093, China.

matching mode are studied. On this basis, a wideband RFID anti-metal tag antenna is designed. The changing characteristics of the chip's impedance and antenna's impedance tend to be consistent, achieving better broadband coverage and impedance matching. According to the metallic surface test experiment, the reading range of the tag antenna reaches 4.5 m. Through simulation and performance testing, it is found that the return loss of the antenna is very low, and its gain is high in a wide frequency range, thus verifying the feasibility of module matching for impedance matching in a wide frequency band.

2. STRUCTURE OF THE TAG ANTENNA

A novel tag antenna is presented using a hybrid microstrip and coplanar waveguide (CPW) structure. The antenna is attached to the front of a single-layer 1.6 mm FR4 substrate with a dielectric constant of 4.4 and dielectric loss tangent of 0.02. The antenna uses an arc microstrip feedline to produce the 10-dB effective bandwidth, which covers the UHF working frequency band of 820 $\sim$ 980 MHz. By adjusting the asymmetrical arc microstrip transmission feedline, the impedance can be adjusted to achieve impedance module matching in a wider frequency band. As shown in Figure 1, the overall structure of the proposed antenna is a ring with an inner diameter $R_1 = 15$ mm and outer diameter $R_2 = 25$ mm.

Two asymmetrical arc-shaped slots are inserted inside and outside the ring by etching, for which extending the length of the microstrip transmission line reduces the size of the antenna. By adjusting the asymmetric microstrip feedlines formed by arc-shaped slots, the dual frequency band generated by the asymmetric structure is converted into a wide frequency band with a center frequency of 920 MHz. The angles θ_1, θ_2, and widths W_1, W_2 of the two arc-shaped slots are adjusted respectively to modify the structure of the microstrip feedline. To further illustrate the influence of the angle of the arc slot on the antenna impedance, Figure 3 shows the effect of θ_2 on the real and imaginary parts of the antenna impedance. The results show that different angles have obvious effects on the real and imaginary parts of the antenna impedance. When θ_2 is 120°, the impedance change of the antenna tends to be stable. Through HFSS simulation, it is found that θ_2 has a great influence on the imaginary part of the impedance of the antenna. When θ_2 is gradually reduced, the imaginary part of the impedance will gradually increase until it becomes a positive value. As shown in Figure 1(b), inserting a u-shaped patch in the middle of the arc-shaped microstrip feedlines, the distance between the microstrip lines is 0.1 mm. The arm's length, arm's width, and bottom width are L_4, W_4, W_5, and by modifying these parameters to adjust the real and imaginary parts of the impedance accurately, the input impedance can be easily adjusted without an additional complicated matching network to achieve the impedance module matching. As shown in Figure 1(c), since a metal layer is coated on the back of the dielectric material, the antenna can maintain its excellent performance even if it is located in an environment where metal objects are present, and it can maintain its excellent performance. As shown in Table 1, the structural parameters of the proposed antenna include 16 items.

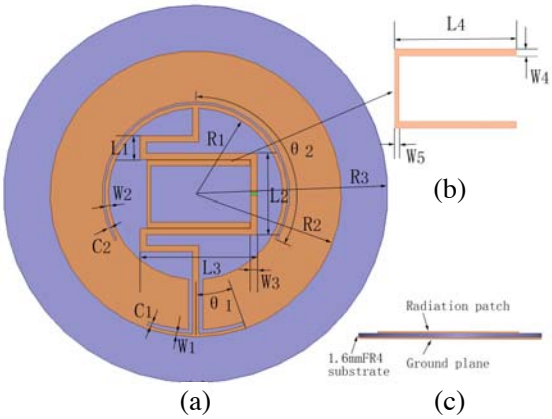

Figure 1. Structure of the proposed antenna. (a) Top structure. (b) U-shaped patch. (c) Elevation view.

Table 1. Parameters of proposed antenna.

W_1	W_2	W_3	W_4	W_5	C_1	C_2	L_1
0.6 mm	0.7 mm	1.1 mm	1 mm	0.6 mm	0.7 mm	0.4 mm	4.1 mm

L_2	L_3	L_4	R_1	R_2	R_3	θ_1	θ_2
14.2 mm	20.1 mm	17.7 mm	15 mm	25 mm	33 mm	20°	120°

Figure 2 shows the antenna matching design process. As shown in Figure 2(a), based on the ring-shaped patch antenna, two symmetrical arc-shaped grooves are etched on its surface, and the working frequency is not at the expected frequency. Next, as shown in Figure 2(b), adjust the length and width of the center microstrip to increase its imaginary part. The impedance matching at this time is similar to T-matching, and the imaginary part of the antenna impedance is positive ($1.37 + j209\,\Omega$), which is in common with the conjugate matching, then add impedance transformation section to adjust the real part of the impedance. It was observed in the design process that when the position and length of the two arc-shaped grooves are adjusted, the imaginary part of the impedance can be changed to a negative value, but the real part is still small. The structure is further adjusted, as shown in Figure 2(c). The resonance shifts to 0.91 GHz at this time, and the dual-band formed by the asymmetric structure will produce a peak at 0.83 GHz, which reduces the bandwidth of the antenna. As shown in Figure 2(d), by adjusting the microstrip structure, the dual-frequency band is transformed into a wide frequency band. At this time, a u-shaped patch is added to accurately adjust its impedance matching. Increasing the real part of the impedance reduces the imaginary part of the impedance and can expand the bandwidth of the antenna.

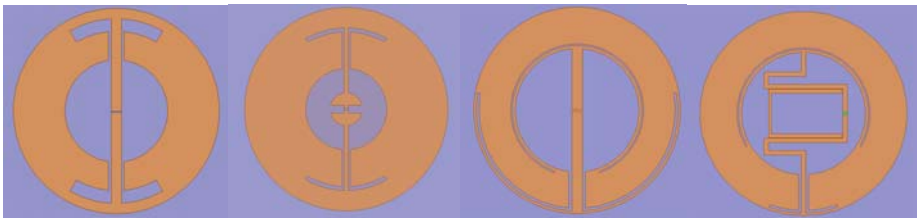

Figure 2. Intermittent tag configurations in the matching design process. (a) Configuration A. (b) Configuration B. (c) Configuration C. (d) Configuration D.

As shown in Figure 4, the fabricated prototype of the tag antenna is verified by experiments. The impedance module matching mode is applied to the broadband anti-metal RFID tag antenna. The experimental scheme proposed in [11] is used to connect the tag antenna to the two ports of a vector network analyzer (Agilent E8363B) through probes. Port extension technology is used to eliminate the influence of the test fixture. According to the return loss (S_{11} parameter) of the experimental test, relevant data can be extracted to calculate the impedance of the tag antenna.

3. ANALYSIS OF THEORY AND RESULTS

3.1. Module Matching of Tag Antenna

Module matching is a matching mode that enables the load (tag chip) to obtain maximum power from the source power (the induced voltage source of the tag antenna). According to Thevenin's theorem, a complex circuit can be equivalent to a conversion circuit with a single impedance and ideal voltage source connected in series [12]. At this time, the chip impedance and antenna impedance are considered as a whole for calculation.

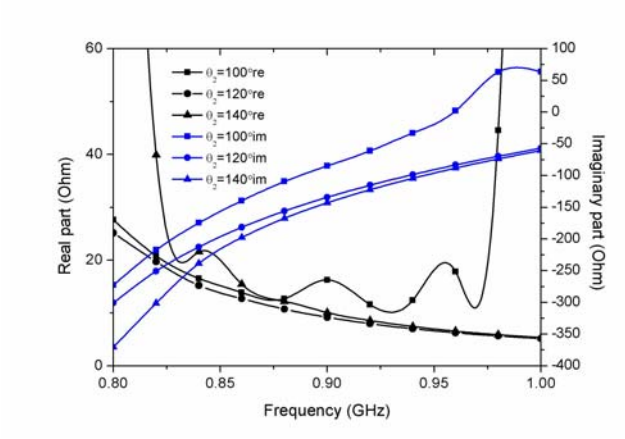

Figure 3. The influence of θ_2 on the real and imaginary parts of impedance.

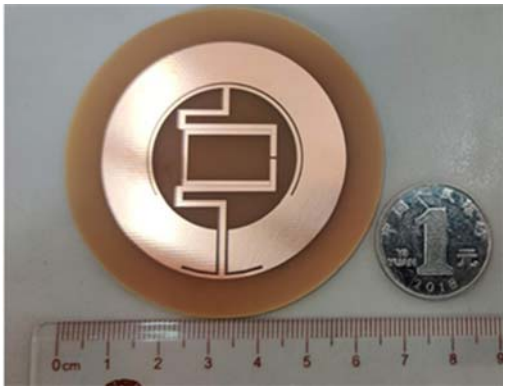

Figure 4. Photograph of the fabricated antenna.

Parameter Z_L is the impedance of the tag chip, and Z_S is the impedance of the tag antenna. The power acquired by the tag chip is calculated by Equation (1).

$$P_L = I_L^2 \cdot R_L = \frac{U_S^2}{(R_S + |Z_L|\cos\theta_L)^2 + (X_S + |Z_L|\sin\theta_L)^2} \cdot |Z_L|\cos\theta_L = \frac{U_S^2 |Z_L|\cos\theta_L}{|Z_L|^2 + 2|Z_L| \cdot |Z_S|\cos(\theta_L - \theta_S) + |Z_L|^2} \tag{1}$$

Formula (1) shows that when $|Z_L| = |Z_S|$, the maximum power obtained by the load can be calculated using Equation (2).

$$P_{\max} = \frac{U_S^2 \cos\theta_L}{4|Z_L|} \tag{2}$$

For the same circuit, based on Equation (2) and the maximum power calculation formula for conjugate matching, the maximum power obtained by the load in the case of module matching is less than the maximum power in conjugate matching. However, for wideband RFID tag antennas, most research results show that impedance conjugate matching in a wideband is limited to a small part of the frequency range, and its transmission efficiency is only about 50%. At the same time, since the real and imaginary parts of the chip impedance will change in different frequency ranges, it is difficult to extend the impedance matching to the entire wide frequency band. Therefore, although the existing tag antenna can work in a wide frequency range, the impedance matching effect in some frequency bands is very poor, and even a dead zone occurs [13]. As far as the impedance matching mode of the tag antenna is concerned, the module matching is a better solution for the wideband RFID tag antenna.

In addition, the study found that in the module matching, the changing trend of impedance between the tag and antenna can be adjusted to synchronize, and the real and imaginary parts of the impedance are further adjusted to achieve a mode of impedance matching in a wider frequency band, which is challenging to succeed in the conjugate matching mode.

As shown in Figure 5, the experimental data of the tag antenna's impedance and the impedance of the tag chip (Impinj MonzaR6, 915 MHz threshold power −16.7 dBm [14]) are compared. It can be seen that the real and imaginary parts of the impedance change trend are synchronized through the analysis of their changes, which verified that the changing trend of the two in the module matching mode is consistent so that it is easier to achieve impedance module matching in a wide frequency band.

It is worth noting that this article is still defined by the traditional reflection coefficient and return loss. Figure 4 shows that the antenna's complex impedance at 0.92 GHz on the metal surface is very close to the chip's impedance, and both have a high capacitance imaginary part and a small real part. This is because the impedance target is to achieve $|Z_L| = |Z_S|$ when the tag antenna is designed by the module matching. At the port, the setting of the complex impedance is different from the conjugate matching.

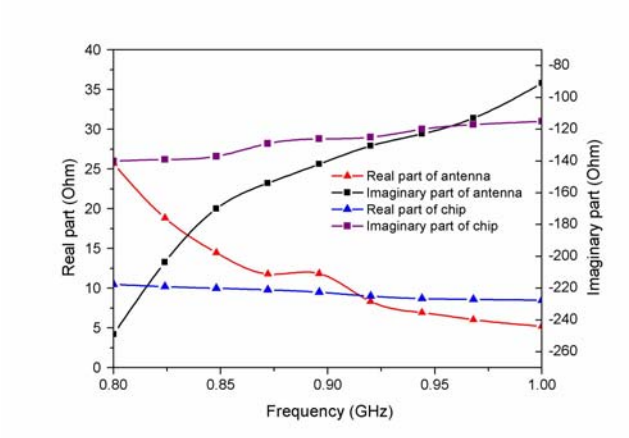

Figure 5. Comparison of measured tag antenna impedance and chip impedance.

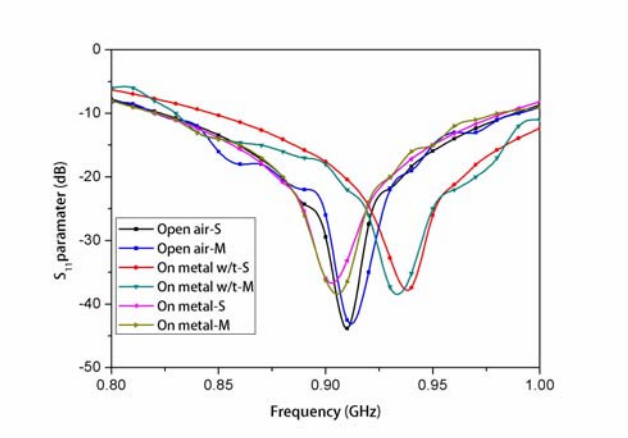

Figure 6. Measured and simulated return loss of the proposed antenna in different environments (* M: measured, S: simulated, w/t: without touch).

The imaginary part of the antenna's impedance is set to $-jX$ to correspond to the imaginary part of the impedance of the tag chip. Therefore, when calculating the reflection coefficient of the antenna, the imaginary part of the antenna should be changed to $-jX$.

3.2. Results and Discussion

As shown in Figure 6, simulation and experimental tests were carried out on the S_{11} parameters of the tag antenna. (characterized both in open air and on a metallic plate with a surface of $200 \times 200\,\text{mm}^2$. The suffixes S and M were simulation data and test data; w/t means without touch with metal.) Among them, the test with a distance of 1 mm away from the metal plate is to verify the effect of the label installation on certain internal metal-containing items, such as cigarette cases. Obviously, in the three test environments, the S_{11} parameters are less than $-10\,\text{dB}$ in the entire target UHF frequency band, which meets the wideband requirements for tag antennas in most engineering applications. According to the analysis of S_{11} related to metal, the minimum value of S_{11} that is not in contact with the metal surface is shifted to the right by 30 MHz from the S_{11} in the open air, and when the antenna is directly attached to the metal plate, the S_{11} has a small offset. The return loss of the two has increased. Analyzing the impedance matching situation at this time, when the antenna does not touch the metal ground, it is equivalent to increasing the capacitance, reducing the imaginary part of the antenna's impedance, and increasing the frequency of impedance matching, which causes the return loss to shift to the right. When the antenna is directly attached to the metal surface, it will only cause a slight change in the current of the antenna, and its impedance will also change accordingly. Therefore, the frequency band shift caused by it is much smaller than the case of non-contact. At the same time, due to the existence of lumped elements tolerances, there is a certain difference between the return loss of the simulation test and the measured value.

As shown in Figure 7, the gain parameters of the tag antenna were simulated and experimentally tested. The antenna gain was measured under the condition of minimum tag turn-on power. Place the reader antenna and tag in the anechoic room with linear polarization and a fixed distance of 1 m. The test environment was in open air and directly attached to a $200 \times 200\,\text{mm}^2$ metal plate. Due to the effect of reader antenna loss, the simulated test value is higher than the experimental test value. When the tag antenna is placed on a metallic surface, its gain is increased by 5 dB. Since a larger metal plate will increase the current area of antenna, it will help to increase the gain of the tag antenna. Figure 7(b) shows the gain of the tag in the open air and on metal plates of different sizes. When the size of the plate is larger than $200 \times 200\,\text{mm}^2$, the gain can be maintained above $-6\,\text{dB}$ near the UHF center frequency band. In the entire UHF operating band, the peak radiation efficiency of the tag antenna is 6%. The poor radiation efficiency is caused by the compact size and low profile of the antenna. When the thickness of the tag antenna is only 1.6 mm, this is an unavoidable problem for

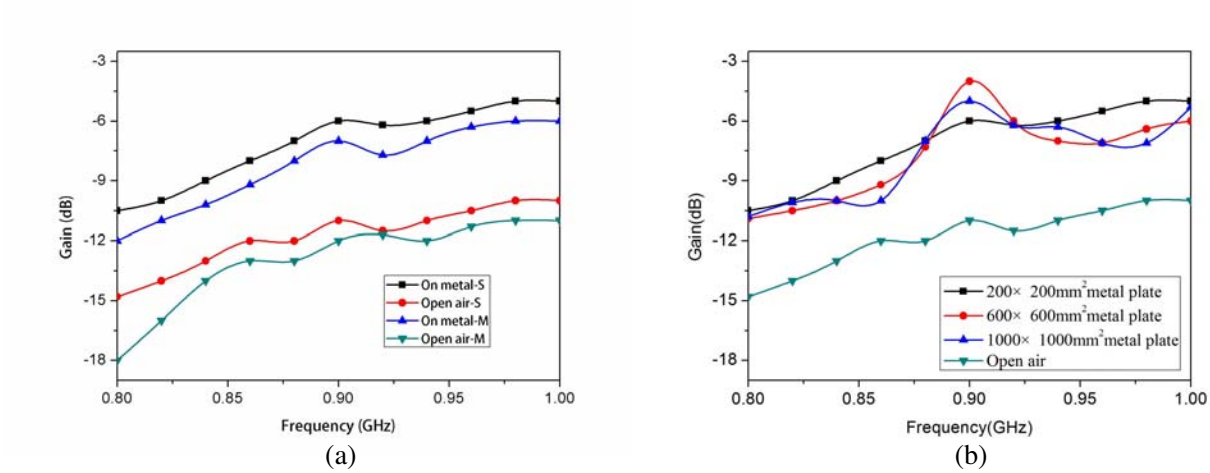

Figure 7. Measured and simulated gain of the proposed antenna in different environments. (a) Measured and simulated gain. (b) Simulated antenna realized gains.

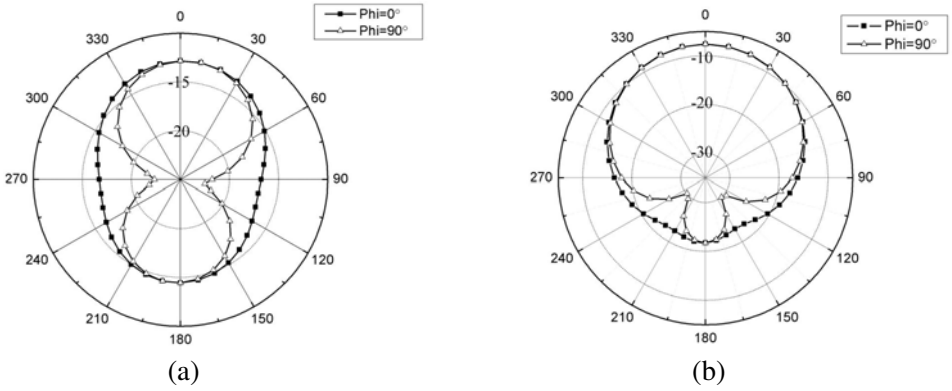

Figure 8. Radiation pattern of antenna in open air and metal plate at 910 MHz. (a) Open air. (b) On metal.

most tag antennas [15].

Figure 8 shows the radiation pattern of the tag placed on the open air and metal plate at 910 MHz. In Figure 8(a), since the metal bottom plate of the tag antenna itself has the same size as the radiation patch, the front and back sides of the tag antenna have extensive radiation, and the H plane has good omnidirectionality. Figure 8(b) shows that adding a large metal floor will have a more significant impact on the radiation pattern of the antenna. The back lobe of the tag antenna is tiny and mainly radiates to the front. In this design, the radiation of the RFID tag antenna concentrates on the microstrip line and both sides of the inner arc groove, instead of the edge of the tag antenna, reducing the influence of the metal floor on the radiation efficiency.

In order to test the identification performance of tag antennas in the UHF bands in Europe, North America, and China, a linear polarization reader (Laird-E9012PLNF, gain 12 dBi) was set to EIRP (equivalent isotropically radiated power) of 3.3 W and 4 W, respectively. The reading distance of the tag antenna was measured with the same EIRP in the open air and metal environment. The maximum reading distance is 2.2 m at 902 MHz in the open air environment and 4.5 m at 910 MHz in the metallic environment. The test results show that the tag antenna has an excellent performance in a metal environment.

As shown in Table 2, the reading performance of the proposed tag antenna is compared with other tag antennas in a metallic environment. The working frequency of the listed tags is all around 910 MHz. Compared with the antenna proposed in [16], the proposed antenna is not as small as it, but the proposed antenna has a better reading performance. In [17], the antenna has a significantly narrow

Table 2. Comparison of antenna parameters between proposed antenna and other antennas.

Ref	Sensitivity (dBm)	Antenna size (mm^3)	Maximum Gain (dB) on metal plate	Maximum reading range(m) on metal plate	Cover the major UHF RFID region bands	Matching model
[15]	−17.4	$70 \times 70 \times 1.6$	−7.96	4.36	No	Conjugate match
[16]	−14	$65 \times 20 \times 1.5$	N.A	3.1	No	Conjugate match
[17]	−16.7	$30 \times 25 \times 3$	−5.6	8.9	No	Conjugate match
[18]	−16.7	$41 \times 18 \times 4.5$	N.A	4.1	No	Conjugate match
Proposed Antenna	−16.7	$R_{33} \times 1.6$	−6.9	4.5	Yes	Module match

bandwidth. At about 910–920 MHz. The performance of the antenna beyond the frequency range will drop rapidly, but its identification distance reaches 8.9 m. The antenna identification distance designed in this article is inferior to the former, but it can cover the main UHF Working frequency. Compared with the antenna in [15] which used vias and specific substrate, the single-layer without a through-hole structure of the proposed antenna reduces the processing cost. Compared with the tag antenna with the conjugate matching mode, such as the commercial tag in [18], the proposed tag antenna using the module matching mode can not only achieve the target of 4.5 m reading distance in the metal environment but also with a smaller size, making it excellent for broadband UHF RFID tag antenna's impedance matching.

4. CONCLUSION

This paper proposes an RFID broadband anti-metal tag antenna based on module matching. Its performance is better than the traditional tag antenna, which uses conjugate matching mode in a metal environment, and the impedance of the antenna is easy to achieve consistent changes, so that it is easier to further achieve a wide frequency band and excellent impedance matching. Furthermore, the simulated and experimental data of the tag antenna show a reading range of 4.5 m in a metal environment, and the working frequency band covers 820–980 MHz, which verifies the superior performance of the tag antenna based on module matching. Simultaneously, the proposed tag antenna also has high engineering application value and is very strong for marking large metallic objects in a wide frequency band.

REFERENCES

1. Xavier, F., O. K. Hikage, M. S. D. P. Pessoa, and A. L. Fleury, "A view about RFID technology in Brazil," *Proc. Technol. Manage. Global Econ. Growth*, 1–9, 2010.
2. Gao, Y., D. Yang, and W. Ning, "RFID application in tire manufacturing logistics," *Proc. 2010 IEEE Int. Conf. Adv. Manag. Sci.*, Vol. 3, 109–112, 2010.
3. Yan, Y., J. Ouyang, X. Ma, R. Wang, and A. Sharif, "Circularly polarized RFID tag antenna design for metallic poles using characteristic mode analysis," *IEEE Antennas Wireless Propag. Lett.*, Vol. 18, No. 7, 1327–1331, July 2019.

4. Chen, W., H. Chen, Y. Lin, and Y. Lu, "A circularly polarized square-ring patch tag antenna mounted on metallic plane," *Proc. 2016 IEEE 5th Asia-Pacific Conf. Antennas Propag. (APCAP)*, 119–120, Kaohsiung, 2016.
5. Lee, Y., B. Chung, E. Lim, and F. Bong, "Miniature slotted-folded-patch antenna for on metal UHF tag," *Proc. 2018 IEEE Asia-Pacific Conf. Antennas Propag. (APCAP)*, 492–493, Auckland, 2018.
6. Ng, W. H., E. H. Lim, F. L. Bong, and B. K. Chung, "Compact planar Inverted-S antenna with embedded tuning arm for on-metal UHF RFID tag design," *IEEE Trans. Antennas Propag.*, Vol. 67, No. 6, 4247–4252, April 2019.
7. Michel, A., et al., "Design considerations on the placement of a wearable UHF-RFID PIFA on a compact ground plane," *IEEE Trans. Antennas Propag.*, Vol. 66, No. 6, 3142–3147, June 2018.
8. Casula, G. A., G. Montisci, and G. Mazzarella, "A wideband PET Inkjet-Printed antenna for UHF RFID," *IEEE Antennas Wireless Propag. Lett.*, Vol. 12, 1400–1403, 2013.
9. Pillai, V., "Impedance matching in RFID tags: To which impedance to match?," *Proc. 2006 IEEE Antennas Propag. Soc. Int. Symp.*, 3505–3508, Albuquerque, NM, 2006.
10. Choudhary, A., D. Sood, and C. C. Tripathi, "Wideband long range, radiation efficient compact UHF RFID tag," *IEEE Antennas Wireless Propag. Lett.*, Vol. 17, No. 10, 1755–1759, Oct. 2018.
11. Qing, X., C. K. Goh, and Z. N. Chen, "Impedance characterization of RFID tag antennas and application in tag co-design," *IEEE Trans. Microw. Theory Tech.*, Vol. 57, No. 5, 1268–1274, May 2009.
12. Sheikholeslami, A., "Thevenin and norton equivalent circuits: Part 3 [Circuit Intuitions]," *IEEE Solid-State Circuits Mag.*, Vol. 10, No. 4, 7–9, Fall 2018.
13. Marrocco, G., "The art of UHF RFID antenna design: Impedance-matching and size-reduction techniques," *IEEE Antennas Propag. Mag.*, Vol. 50, No. 1, 66–79, February 2008.
14. "Impinj monza R6 tag chip datasheet," 2016, [Online] Available: https://support.impinj.com.
15. Pan, T., S. Zhang, and S. He, "Compact RFID tag antenna with circular polarization and embedded feed network for metallic objects," *IEEE Antennas Wireless Propag. Lett.*, Vol. 13, 1271–1274, 2014.
16. Chen, S.-L. and K.-H. Lin, "A slim RFID tag antenna design for metallic object applications," *IEEE Antennas Wireless Propag. Lett.*, Vol. 7, 729–732, 2008.
17. Lee, Y., C. Moh, E. Lim, F. Bong, and B. Chung, "Miniature folded patch with differential coplanar feedline for metal mountable UHF RFID tag," *IEEE Journal of Radio Frequency Identification*, Vol. 4, No. 2, 93–100, June 2020.
18. "UHF monza R6 chip ABS metal resistant label — ABS4118," 2020, [Online] Available: http://www.iotku.com/Product/425721627888582656.html.